Study of the driven damped pendulum: Application to Josephson junctions and charge-density-wave systems

A. H. MacDonald

Division of Physics, National Research Council of Canada, Ottawa, Ontario K1A 0R6, Canada

Michael Plischke

Physics Department, Simon Fraser University, Burnaby, British Columbia V5A 1S6, Canada
(Received 7 June 1982)

The equation of motion of the driven damped pendulum is related at low dissipation to a current-fed Josephson junction and at high dissipation to transport in charge-density-wave (CDW) systems. We report on an extensive numerical investigation of these equations. At low dissipation we find broad bands of chaotic solutions as a function of the frequency and amplitude of the driving force. It is pointed out that periodic solutions may possess a symmetry corresponding to the invariance of the equations of motion under a simultaneous spatial (phase) inversion and a shift in the phase of the driving force by an odd multiple of π. At low dissipation chaos is usually approached via a sequence of period-doubling bifurcations if this symmetry has been broken and directly from period 1 with associated intermittency behavior if the symmetry is not broken. At high dissipation no chaotic behavior is found but broad bands of symmetry-broken solutions, which may be related to recently reported hysteresis phenomena in CDW systems, occur. Discussions of properties of the Poincaré maps and of the fractal dimension of the strange attractors associated with the chaotic solutions have been included.

I. INTRODUCTION

We report on an extensive numerical investigation of the classical equation of motion of the simple pendulum with viscous damping driven by a periodic external force. Our motive for this study is twofold. First, the equation of the pendulum, with a change of variables, applies directly to a current-fed Josephson junction[1] and, with some caveats, to one-dimensional charge-density-wave (CDW) structures such as are found in NbSe$_3$ or TaS$_3$ in the presence of a periodic applied electric field. In both these systems interesting dynamic effects have been reported. In Josephson parametric amplifiers an increase in the amplitude of the oscillatory driving signal may lead to broad-band voltage fluctuations.[2] This noise rise has been ascribed by Huberman *et al.*[3] to the appearance of a strange attractor and associated chaotic behavior for the pendulum equation. In incommensurate CDW systems such as NbSe$_3$ one expects that conduction will occur via the motion of solitons or discommensurations. If the pinning of the solitons is dominated by the Peierls potential[4] a direct connection between the equation of motion of the soliton and the pendulum equation can be established. If, on the other hand,

impurity pinning dominates it may be necessary to add a noise term to the equation of motion. The noise is generated in this case by spatial fluctuations in the potential seen by the soliton during its motion. To date, no chaotic or turbulent motion has been observed in CDW systems. However, Tessema and Ong[5] have recently reported hysteresis in NbSe$_3$ subjected to an ac field and these effects may be connected to the nonlinearity of the equation of motion.

Our second motivation for studying this problem originates in the recent advances that have been achieved in the study of nonlinear dynamical problems.[6] In many systems, the onset of chaotic or turbulent motion can be explained in terms of the properties of simple one- or two-dimensional Poincaré maps. What is not clear yet is whether or not a differential system can always be converted into a simple analytic Poincaré map without loss of some basic features, although some striking successes have been achieved[7,8] in this task. We have made an extensive investigation of the Poincaré map generated by the differential equation of the pendulum and find that the initial onset of turbulence with increasing force in this system falls most often into one of two classes depending on the parameters of

the system. Over one range of frequencies we find that chaos is preceded by a Feigenbaum sequence of period-doubling bifurcations.[6,9] For another range of frequencies the onset is best described by a Manneville-Pomeau scenario[6] although the transition in our case seems to be directly from period 1 to chaos without any intermediate period-3 regime. However, for some parameters we have observed transition to chaos via more complicated periodic sequences such as period $1 \rightarrow$ period $3 \times 2^n \rightarrow$ chaos.

In the chaotic regime we have calculated the fractal dimension of the strange attractor both by direct bin counting and through a conjectured relation[10] to the Lyapunov exponents. We find, for the range of parameters studied most closely that the fractal dimension is near 1, indicating that the strange attractor is nearly one dimensional. Nevertheless, we have not succeeded in finding an analytic form for a one- or two-dimensional map that reproduces all essential features of the system, either in the chaotic regime or through the approach to chaos.

The structure of this paper is as follows. In Sec. II we connect the pendulum equation with the physical systems mentioned above. Section III contains the bulk of our numerical results including some approximate phase diagrams, selected phase plots, and power spectra of the solution. In Sec. IV the Poincaré map generated by the differential equation is described for specific parameters and attempts to find corresponding one-dimensional maps are discussed. Section V contains a discussion of the strange attractors that occur in the chaotic regime and evaluations of their fractal dimensions. Finally, Sec. VI contains some concluding remarks and suggestions for further work.

II. RELATION OF THE PENDULUM TO OTHER PHYSICAL SYSTEMS

We note the following.

(a) The McCumber model[1] for a current-fed Josephson junction has the following equivalent circuit equation:

$$\frac{hc}{2e}\left[\frac{d^2\phi}{dt^2} + \frac{1}{R_J C}\frac{d\phi}{dt} + \frac{2eI_0}{hc}\sin\phi\right] = I_{rf}\cos\omega_d t \ ,$$

$$(1)$$

where ϕ is the phase difference between the superconductors, R_J and C are the junction resistance and capacitance, respectively, I_0 is the critical supercurrent, and I_{rf} is the amplitude of an external microwave field of frequency ω_d. The junction current and voltage are given in terms of ϕ by

$I_J = I_0\sin\phi, V = (h/2e)d\phi/dt$. Making a few changes of variables we obtain the equation in the standard form which we use below,

$$\frac{d^2\phi}{d\tau^2} + R\frac{d\phi}{d\tau} + \sin\phi + F_0\cos 2\pi\omega\tau \ ,$$

with

$$R = \left[\frac{h}{2R_J^2 CeI_0}\right]^{1/2} \ ,$$

$$F_0 = \frac{I_{rf}}{I_0} \ ,$$

$$(2)$$

and

$$\omega = (\omega_d/2\pi)\left[\frac{hC}{2eI_0}\right]^{1/2} \ .$$

Typical values[1] of the dimensionless resistance R seem to lie in the range $0.03 - 0.7$ indicating that these systems will be underdamped in the linear regime.

(b) A commensurate CDW such as is found in TaS_3 is pinned to the underlying lattice.[11] In an applied electric field the CDW will, to a first approximation, move as a unit and be subject, in a one-dimensional system, to a potential of the form $V_0[1 - \cos(2\pi/a)X]$ plus higher harmonics where a is the lattice spacing and X a specific point on the CDW. Associating a mass M with the CDW and an effective charge e^* coupling the CDW to an external field we may immediately write down the equation of motion

$$M\frac{d^2X}{dt^2} + \frac{1}{\tau}\frac{dX}{dt} + \frac{2\pi}{a}V_0\sin\frac{2\pi}{a}X = e^*E(t) \ ,$$

$$(3)$$

which can be transformed into our standard form (2). Here τ is a phenomenological damping coefficient.

If the CDW is incommensurate ($NbSe_3$) one expects that conduction will occur via the movement of solitons or discommensurations. Solitons can be pinned either by impurities[12] or by a Peierls potential due to the periodic background.[4] The Peierls potential takes the form $V_P[1 - \cos(2\pi x/a)]$ in the simplest approximation; the impurity potential presumably has some spatially fluctuating component as well as an average periodic component. If we ignore the fluctuating component we again arrive at an equation of the form (3), this time for the soliton dynamics. It is difficult to estimate the effective damping parameter R for such materials but

existing data[13,14] indicate that such systems are overdamped ($R > 2$) in the linear regime.

III. NUMERICAL RESULTS

We have integrated the differential equations [Eqs. (2)] for several different values of R and in each case a large number of F and ω values using a predictor-corrector method. We present results here mainly for $R = 0.5$ which is a reasonable value for Josephson junctions and small enough that a wide range of interesting results are obtained. Below we shall also comment on the overdamped case which is more appropriate for charge-density wave systems. Figure 1(a) displays the phase diagram for $R = 0.5$ for a specific choice of initial conditions, i.e., $\phi(0)=0$, $\dot{\phi}(0)=0$. The reason for this consistent choice is that in some regions of parameter space different limit cycles coexist with interwoven
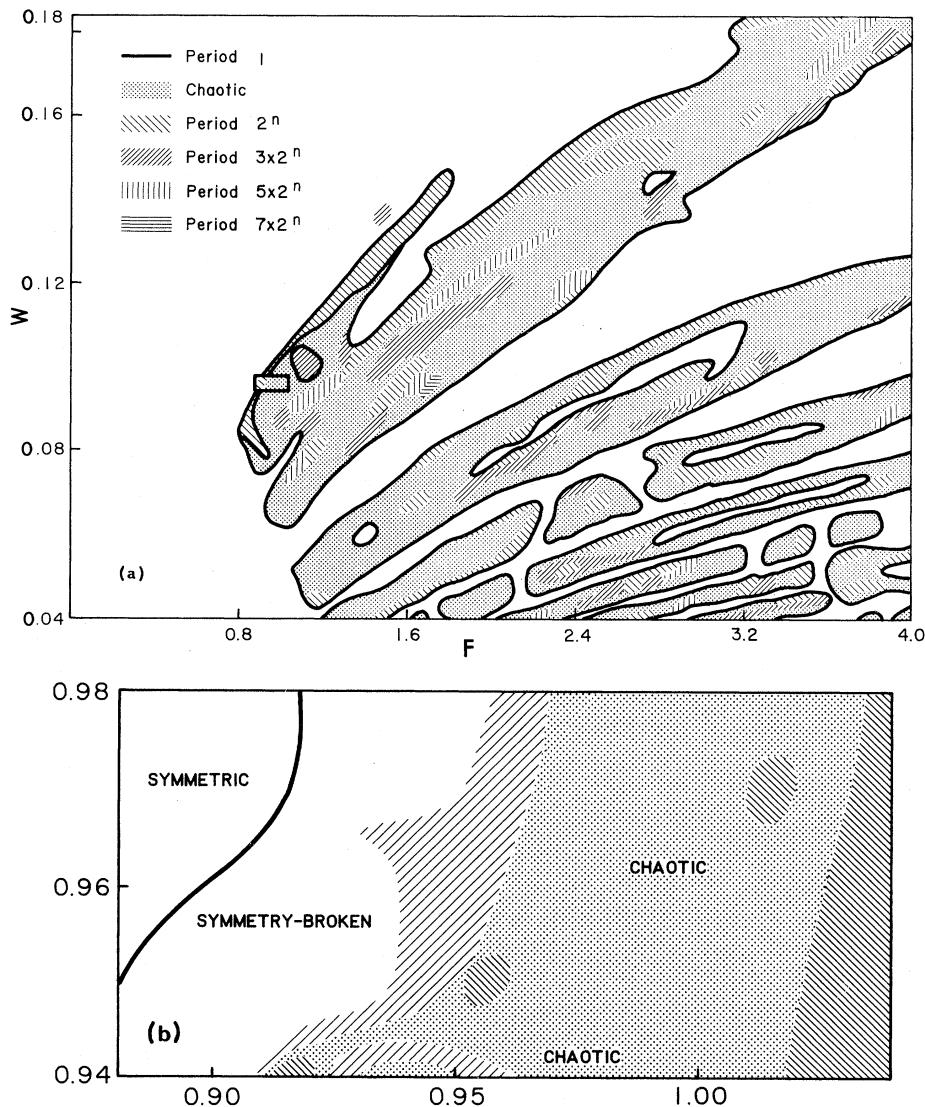

FIG. 1. (a) Regions of various types of limit cycles in a plane in F,ω space at $R = 0.5$. This figure was generated by examining $\sim 2 \times 10^3$ points on a regular grid in the region illustrated. If no periodic solution was evident after 200 cycles of the driving force, the point was assumed to be associated with chaotic behavior. Each point was assumed to be representative of a small surrounding square in parameter space. As shown by the behavior in (b) this assignment can misrepresent small regions and, in particular, the approach to chaos may sometimes on closer examination turn out to be different from what is indicated here. Note in (b) that the period-doubling bifurcation approach to chaos is preceded by a breaking of symmetry in the period-1 solutions which is discussed below.

basins of attraction. In particular, the approach to chaos in this system is sometimes dependent not only on the externally controllable parameters but also on the initial conditions. An average over an ensemble of initial conditions would produce a slightly expanded region in the F-ω plane in which solutions with periodicity different from that of the driving force are found. A few general comments are in order. The region inside the bounding curves cannot be fully characterized by a numerical study of the differential equation. Dramatic changes of behavior occur for very small changes of the parameters including such transitions as trapped chaotic $\rightarrow$ propagating chaotic $\rightarrow$ propagating periodic $\rightarrow$ trapped periodic. Our results seem to show that these is no interval in either F or ω in the chaotic regime which is entirely free of periodic solutions. This sort of behavior is expected on the basis of what is known to occur for one-dimensional maps on the interval. As is shown below for a specific choice of ω, very different limit cycles are extremely close together in parameter space and it is expected that much of the smaller scale structure of the region must be missed in any numerical study. [Compare Fig. 1(a) and Fig. 1(b).] The largest periodic section of the enclosed regime seems to be taken up by states of period 1. States of period 2^n and 3×2^n are also common and some regions where these types of solutions occur are indicated in Fig. 1. On the upper side of the enclosed region we find that a narrow strip of period 2^n solutions bounds the chaotic regime for most values of the force. As the force is increased at constant frequency a sequence of period-doubling bifurcations with the universal Feigenbaum properties[9] precedes chaos. We emphasize that this region is often very narrow: at $\omega = 0.09$ the entire period-doubling cascade occurs over a range of forces $F_\infty - F_2 \simeq 0.0085$. Moreover, we find that in some regions on the upper side chaos can set in in other ways. At $F = 1.4$ we find that as the frequency is lowered the sequence $T = 1 \rightarrow$ chaos $\rightarrow T = 25 \rightarrow T = 7$ occurs in the frequency range $0.1270 - 0.1268$. Alternatively, in a region around $F = 1.6$ the sequence $T = 1 \rightarrow T = 3 \times 2^n \rightarrow$ chaos occurs as the frequency is lowered.

On the low-frequency side of the bounding region we find that the chaotic states normally adjoin the period-1 states without a transition region. The period-1 fixed point simply disappears as a critical value of the force is reached and intermittent behavior[6] is seen. Throughout the chaotic regime confined [i.e., $\phi(t)$ bounded] and propagating [$\phi(t \rightarrow \pm \infty) \rightarrow \pm \infty$] states coexist and it seems to

be impossible to segregate them to different regions of parameter space.

We now exemplify some of this behavior by displaying in some detail results for $\omega = 0.09$. The period-doubling cascade begins at $F = 0.8835$ and period 32 is reached at $F = 0.891\,38$. In this region ϕ is bounded and a typical phase plot for $T = 4$ is shown in Fig. 2(a). $F = 0.8920$ corresponds to a confined chaotic state [Fig. 2(b)]. At $F = 0.91$ the chaotic state propagates but executes a substantial number of orbits in a single well before hopping to the next well [Fig. 2(c)]. AT $F = 0.95$ a periodic propagating solution of period 4 emerges [Fig. 2(d)]. For $F = 0.96$ the solution has period 10 and is propagating, for $F = 0.97$ [Fig. 2(e)] the solution is a confined period-9 state. After an interlude of propagating chaotic behavior a confined period-3 state emerges at $F = 1.0$.

In Figs. 3(a)–3(f) we display the function $\ln |V(\omega)|$ with

$$V(\omega) = \frac{1}{\tau} \int_0^\tau dt \, e^{i\omega t} \dot{\phi}(t) \dot{\phi}(0)$$

(where τ is typically of the order of 100 periods of the driving force) for a number of different values of F at $\omega = 0.09$ and $R = 0.5$. For periodic states τ was chosen to be a multiple of the period. For chaotic states an average over six such intervals has been calculated with different starting conditions. For chaotic states $V(\omega)$ exhibits the usual broadband noise. Note that in the period-doubling cascade the amplitude of successive subharmonics is reduced on average by an amount consistent with Feigenbaum's universal value of 0.82 dB.

Equation (2) possesses an interesting symmetry which plays an important role in characterizing the types of long-time solutions which are possible. To explore this symmetry we define a two-dimensional mapping which describes the propagation of the solution over half a period $(T = 1/\omega)$,

$$\begin{bmatrix} \phi(T(n + \frac{1}{2})) \\ \dot{\phi}(T(n + \frac{1}{2})) \end{bmatrix} \equiv \begin{bmatrix} G_\phi(\phi(nT)), \dot{\phi}(nT) \\ G_{\dot{\phi}}(\phi(nT)), \dot{\phi}(nT) \end{bmatrix} . \qquad (4)$$

Since Eq. (2) is invariant under the change of variables $\phi \rightarrow -\phi$, $\tau \rightarrow \tau + T/2$ the Poincaré mapping for a full period may be expressed in terms of G_ϕ and $G_{\dot{\phi}}$ by
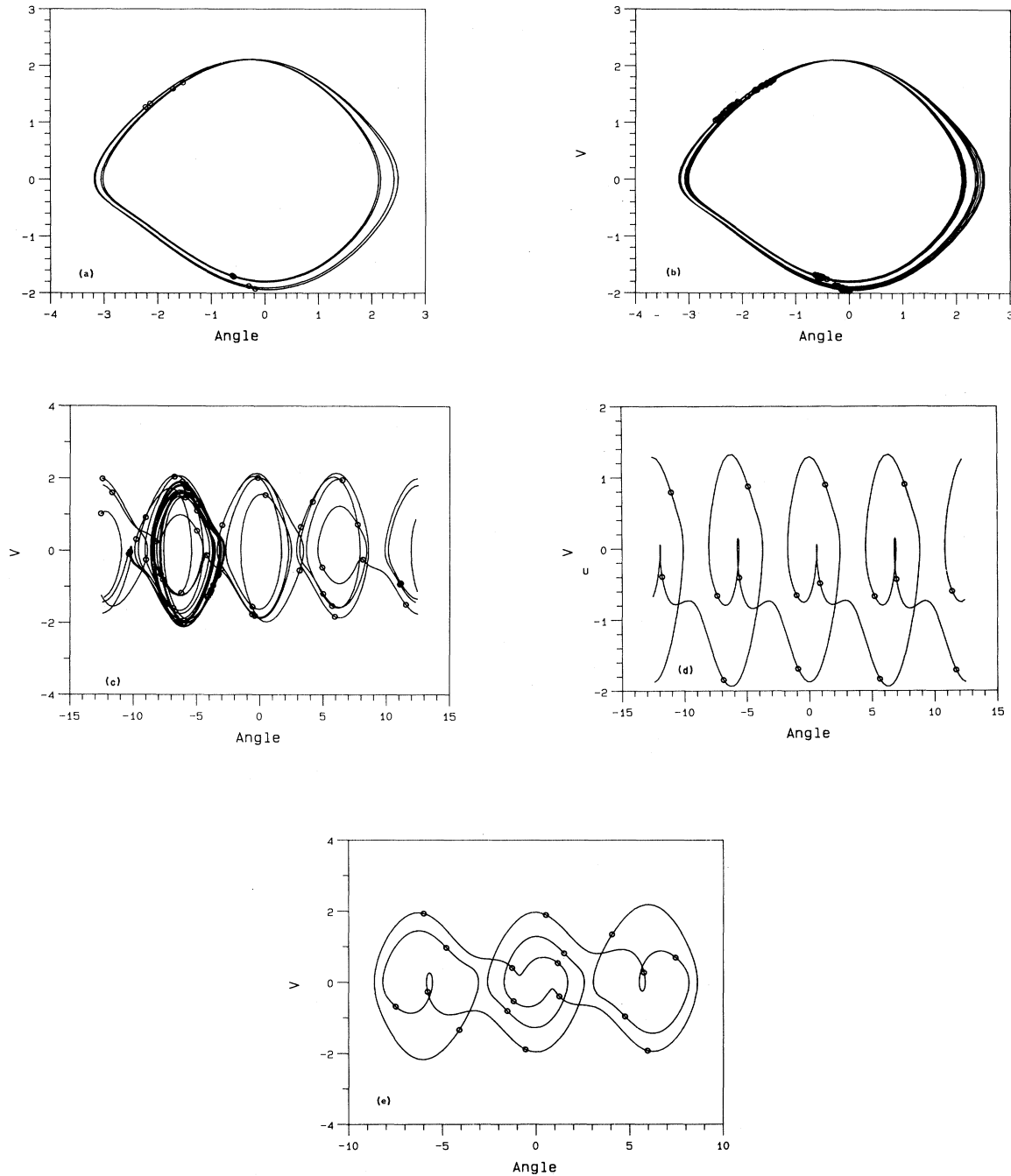
FIG. 2. Phase-space trajectories for the limit cycles at various values of F at $\omega = 0.09$ and $R = 0.5$. The trajectories plotted all begin after 200 cycles of the driving force with a starting condition $\phi(0), \dot{\phi}(0) = 0$. Solutions covering more than four wells are illustrated by plotting ϕ modulo 8π. The circles indicate points separated by half a cycle of the driving period along the trajectory. (a) Bounded period-4 solution at $F = 0.89138$. (b) Bounded chaotic solution at $F = 0.8920$ reached after the period-doubling bifurcations are completed. (c) Propagating chaotic solution at $F = 0.91$. The motion of ϕ here is truly propagating and not diffusive in that the number of "wells" passed increases approximately linearly with time. (d) Propagating period-4 solution which emerges from the chaos at $F = 0.95$. (e) Confined period-9 solution at $F = 0.97$ covering three wells.
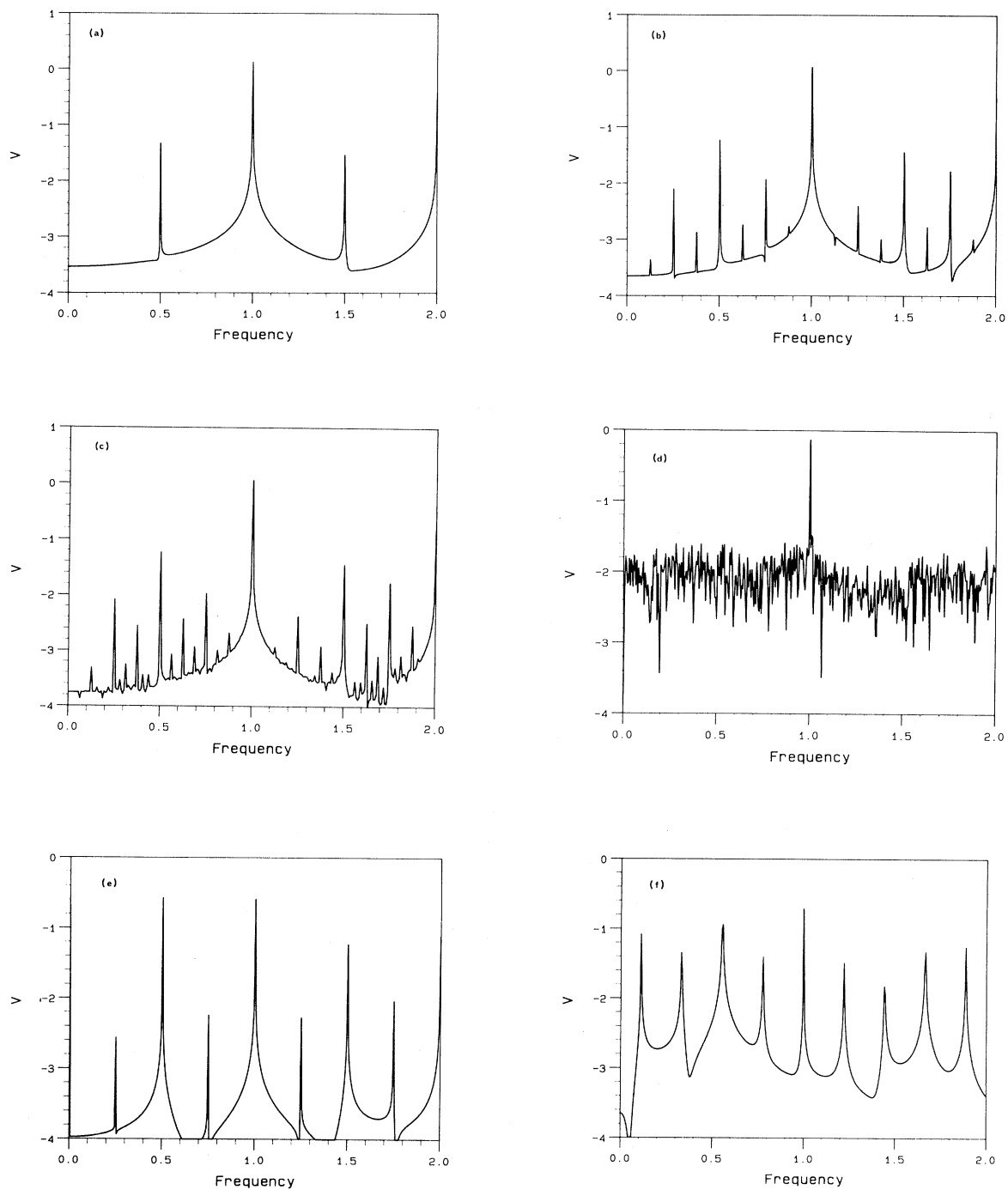
FIG. 3. Fourier transform of the phase velocity for various values of F at $\omega = 0.09$ and $R = 0.5$. The $\log_{10}$ of $V(\omega)$ has been plotted and ω is in units of the driving frequency. (a) Period-2 solution at $F = 0.887$. (b) Period-8 solution at $F = 0.8915$. (c) Period-32 solution at $F = 0.89179$. (d) Chaotic solution at $F = 0.91$. (e) Propagating period-4 solution at $F = 0.95$ (note the peak at $\omega = 0$). (f) Trapped period-9 solution at $F = 0.97$. Note the absence of peaks at even multiples of the basic frequency.

$$
\begin{bmatrix} \phi(T(n+1)) \\ \dot\phi(T(n+1)) \end{bmatrix} = \begin{bmatrix} -G_\phi(-\phi(T(n+\tfrac{1}{2})),-\dot\phi(T(n+\tfrac{1}{2}))) \\ -G_{\dot\phi}(-\phi(T(n+\tfrac{1}{2})),-\dot\phi(T(n+\tfrac{1}{2}))) \end{bmatrix}
$$

$$
= \begin{bmatrix} -G_\phi(-G_\phi(\phi(nT),\dot\phi(nT)),-G_{\dot\phi}(\phi(nT),\dot\phi(nT))) \\ -G_{\dot\phi}(-G_\phi(\phi(nT),\dot\phi(nT)),-G_{\dot\phi}(\phi(nT),\dot\phi(nT))) \end{bmatrix}
$$

$$
\equiv \begin{bmatrix} P_\phi(\phi(nT),\dot\phi(nT)) \\ P_{\dot\phi}(\phi(nT),\dot\phi(nT)) \end{bmatrix} . \tag{5}
$$

Note that any point in phase space satisfying $G_\phi(\phi,\dot\phi)=-\phi$, $G_{\dot\phi}(\phi,\dot\phi)=-\dot\phi$ will be a fixed point of the Poincaré map. We refer to periodic solutions corresponding to these fixed points as symmetric fixed points. Over much of parameter space the long-time periodic solutions do possess this symmetry. For example, the confined period-9 solutions illustrated in Figs. 2(e) and 3(f) have a related symmetry except that here the basic period is $T=9/\omega$. This is signaled in Fig. 3(f) by the fact that all even harmonics of the basic frequency are missing. Note that there is no corresponding symmetry available for even-period solutions.

The symmetry possessed by periodic solutions also has a relation to the nature of the approach to chaos. It is easy to show that at symmetric fixed points of the Poincaré mapping, the eigenvalues of the Jacobian matrix are the squares of the corresponding eigenvalues for the half-period mapping. Since these eigenvalues are real near the chaotic regime, those of the Poincaré mapping cannot reach the value -1, usually associated with the period-doubling bifurcations of the Fiegenbaum scenario. We have, in fact, observed that regions of chaotic solutions can be approached via a sequence of period-doubling bifurcations only if the symmetry of the solutions is first broken. For example, at $\omega=0.075$ where period 1→ chaos with associated intermittent behavior, the solution just outside the chaotic regime is symmetric. This symmetry is signaled in the Fourier transform (see Fig. 4) by the absence of a response component at twice the driving frequency. On the other hand, on the high-frequency side where period-doubling bifurcations occur, symmetry breaking takes place before chaos is approached.

Before discussing the Poincaré maps we comment on the overdamped situation ($R \geq 2$) which may be relevant to charge-density-wave transport. In disagreement with the speculations of Huberman

et al.,[3] we find no solutions with periodicity differing from that of the driving force and, in particular, no chaotic behavior. We do, however, find that as in the underdamped case, regions of symmetric and nonsymmetric solutions exist. Typical results, for the case $R=5.0$, have been illustrated in Fig. 5. It is worth pointing out that it is possible to define an order parameter,

$$\psi=\phi(nT)+\phi((n+\tfrac{1}{2})T) ,$$

and a symmetry-breaking field h [a dc force in Eq. (2)] in association with these solutions. Both the order parameter ψ and a susceptibility $X=\partial\psi/\partial h$ behave in a mean-field-like manner at points of symmetry-breaking "phase transitions." This aspect of the solutions to the driven damped pendulum clearly has a broader significance and will be discussed in more detail elsewhere.[15]
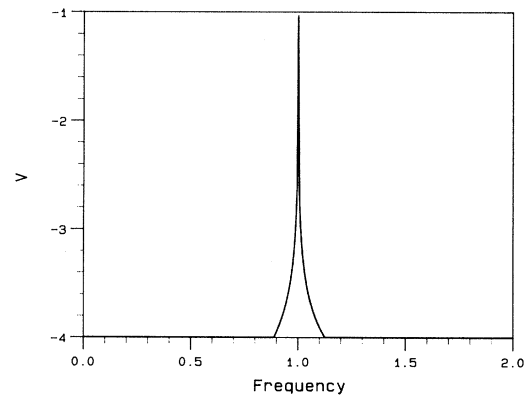

FIG. 4. Fourier transform of the phase velocity for the symmetric period-1 solution on the edge of chaos at $\omega=0.075$, $R=0.5$. (These results are for $F=0.9024$. The solution at $F=0.90245$ is already chaotic.) Note that, unlike the periodic solutions approaching chaos at $\omega=0.09$ [Figs. 3(a)—3(c)] , this solution has no peak in the Fourier transform at even multiples of (in particular twice) the driving frequency.
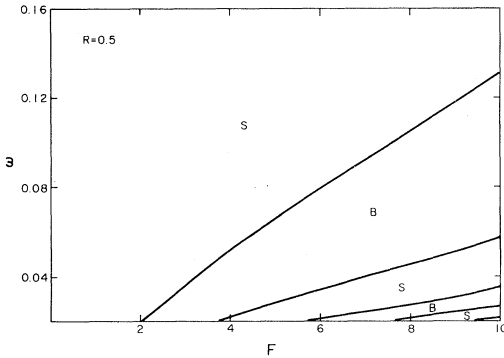
FIG. 5. Regions of symmetric (S) and symmetry-broken (B) solutions in F,ω space at $R=5.0$. All solutions have period $1/\omega$ in this highly damped case.

As mentioned earlier Tessema and Ong[5] have recently observed hysteresis in the CDW system NbSe$_3$ when subject to an ac electric field. It is clear that whenever a periodic long-time solution to Eq. (2) does not have the symmetry

$$\phi(t+T/2)=-\phi(t) ,$$

$$\dot{\phi}(t+T/2)=-\dot{\phi}(t) ,$$

there must be (at least) two different long-time solutions. The solution reached will depend in a complicated way on the starting conditions. From Fig. 5 it is apparent that for overdamped systems many separate regions of symmetry-broken solutions exist. We would like to suggest that the hysteresis in CDW systems could be related to symmetry-breaking phenomena, in the above sense. This suggestion could be investigated by correlating the hysteresis behavior with the dc response in the presence of the ac driving force.
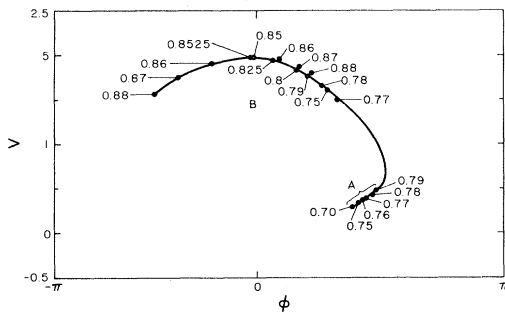

FIG. 6. Movement of the period-1 fixed point of the Poincaré map corresponding to the driven-damped-pendulum equation as a function of F for $R=0.5$ and $\omega=0.09$ and 0.075.

IV. POINCARÉ MAPS

We have examined the behavior of the phase point $\vec{X}_n=(\phi(nT),\dot{\phi}(nT))$ as a function of n for a number of different parameters. Figure 6 shows the movement of the period-1 fixed point as a function of F for $\omega=0.09$. We have found that in this region of parameters the point $\vec{X}_n$ very rapidly, in perhaps three or four iterations, moves to the curve containing the fixed points and then propagates along the curve toward the fixed point. For some values of the force, two different period-1 fixed points corresponding to the two different solutions in the symmetry-broken regime may be reached from different starting points. The first period-doubling bifurcation occurs at $F=0.8835$ and the period-2 fixed points lie along the curve drawn through the period-1 fixed points. Similarly, the period-4,-8,..., fixed points lie along this curve. When the strange attractor appears it first begins to fill out a section of the arc as is shown in Fig. 7(a) for $F=0.90$ but at $F=0.91$ [Fig. 7(b)] it has already developed a strongly two-dimensional character. Its fractal dimension is still close to 1 (~ 1.19, see below); nevertheless it is clear that in terms of the variables $(\phi,\dot{\phi})$ only a fully two-dimensional mapping will provide an adequate representation of the motion.[16]

It seems quite probable that for the interval $0<F\lesssim 0.9$ a one-dimensional mapping of the Feigenbaum type in terms of a variable that measures distance along the curve shown in Fig. 6 will provide a reasonable description. We have not attempted to construct such a mapping, partly because it cannot be valid [Fig. 7(b)] far beyond the onset of chaos and partly because at lower frequencies no period-doubling bifurcations occur at all.

For $\omega=0.075$ the period-1 fixed point is trapped along a small segment, such as that labeled A, in Fig. 6. As the chaotic regime is approached the phase point $\vec{X}$ traverses the segment A very slowly and only reaches its fixed point after typically several hundred cycles. Chaotic behavior in this case is attained when a fixed point no longer exists on this segment. The phase point $\vec{X}$ then slowly traverses the segment, jumps out for perhaps one or two periods, and then repeats the process. The process is very reminiscent of the Pomeau-Manneville scenario for transition to turbulence via intermittency.[6] Figure 7(c) shows the strange attractor for $F=0.9025$ which is a chaotic case (0.9024 is still period 1). It is evident that the strange attractor already has a two-dimensional character and that the phase point is spending nearly all its time along the
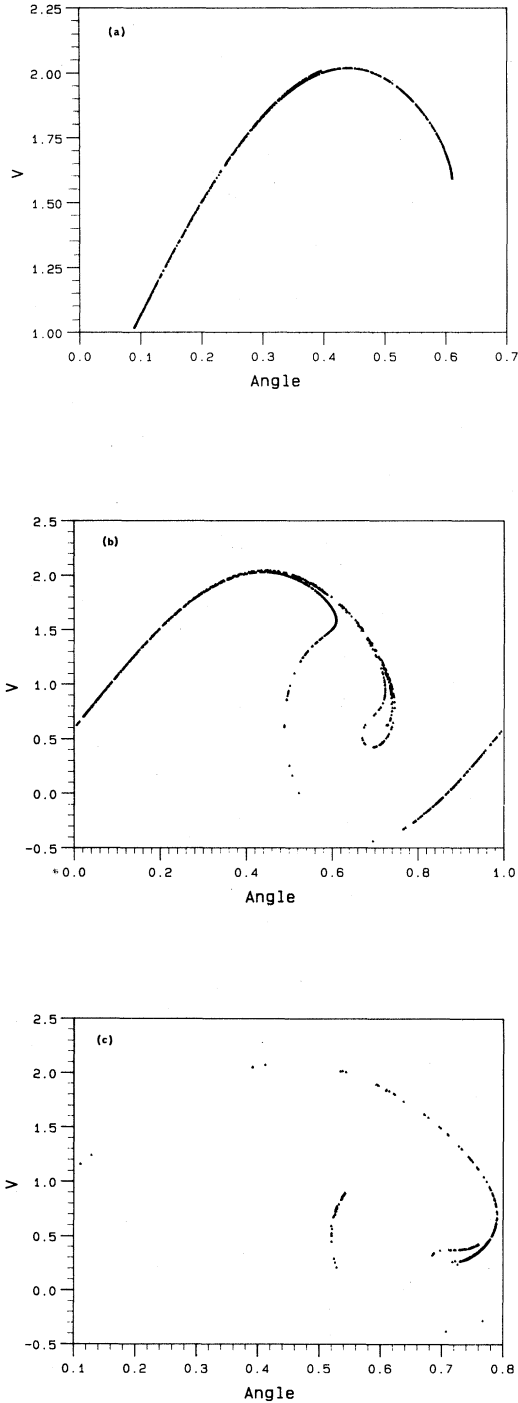
FIG. 7. Representations of the strange attractors associated with chaotic solutions to the equations. These representations were constructed by starting from $\phi(0), \dot{\phi}(0) = 0$ and generating 1000 points in the strange attractor set after eliminating 20 points to remove transient behavior. (a) $\omega = 0.09$, $F = 0.90$. (b) $\omega = 0.09$, $F = 0.91$. (c) $\omega = 0.075$, $F = 0.9025$. The phase points are plotted modulo 2π and the angles are in units of 2π.

short segment A.

We have examined several analytic mappings in an attempt to reproduce the main features of our numerical solutions. Since the system is dissipative a two-dimensional mapping must be area contracting with Jacobian $J = e^{-R/\omega}$. In the linear regime ($F \ll 1$) one can, of course, construct an exact mapping which takes the general form

$$\phi_{n+1} = Fa(R,\omega) + b(R,\omega)\phi_n + c(R,\omega)\dot{\phi}_n \ ,$$

$$(6)$$

$$\dot{\phi}_{n+1} = Fd(R,\omega) + f(R,\omega)\phi_n + g(R,\omega)\dot{\phi}_n \ ,$$

$$(7)$$

where the coefficients $a(R,\omega) \cdots g(R,\omega)$ are all explicitly known. To make this mapping nonlinear we added a term $\lambda \sin\phi_n$ to Eq. (6), $\eta \sin\phi_n$ to Eq. (7). Here η is not independent of λ as we must preserve the value of the Jacobian of the transformation. The resulting mapping is a dissipative generalization of the standard mapping[17] and is very similar to a mapping previously studied by Zaslavsky.[18] We find that this mapping, at least for relatively simple functional dependences of λ on F, does not reproduce the rapid transition to turbulence that we have described above or the shape of the strange attractor. This type of mapping tends to produce a strange attractor with parallel bands, rather than the curved shapes that we observe.

In previous applications of the standard map[17,18] the variables have been the action-angle variables of the unforced, undamped nonlinear problem. We have also produced some Poincaré maps in our chaotic regime in terms of these variables but again find a very complicated shape for the strange attractor rather than the simple parallel bands produced by (6) and (7).

V. FRACTAL DIMENSION OF STRANGE ATTRACTORS

We have calculated the Lyapunov exponents for the chaotic states over a range of forces for $\omega = 0.09$ and 0.075 by a method suggested by Benettin et al.[19] One calculates the mean divergence of two points close together in phase space. By assuming that the largest Lyapunov experiment dominates, one obtains an estimate of λ_1 from the expression[19]

$$\lambda_1 = \lim_{n \to \infty} \frac{1}{n\tau} \sum_{i=1}^{n} \ln \frac{|d_i|}{|d|} \ , \tag{8}$$

where d_i is the separation after one period τ of the driving force. The points are initially separated by a distance d and after each iteration a new pair of points is obtained by moving one point toward the other along the straight line joining them until the separation is once again d. The estimate λ_1 is not very sensitive to variations in d or n as long as d is reasonably small, typically less than 2×10^{-3}. For periodic states λ_1 is negative. For $\omega = 0.09$, $R = 0.5$, and $F = 0.892$ (barely chaotic) $\lambda_1 = 0.11$. In the center of the first chaotic stretch of $F = 0.91$, $\lambda_1 = 1.3$. As periodic states are approached, λ_1 decreases again. These numbers are typical for this value of the resistance.

Using a conjecture of Kaplan and Yorke[10] one can extract the fractal dimensional of the corresponding strange attractor. In our notation the fractal dimension is given by

$$d_F = \frac{\lambda_1}{\lambda_1 + R/\omega} + 1 , \qquad (9)$$

and we find that $d_F = 1.019$ for $F = 0.892$, $d_F = 1.189$ for $F = 0.91$, and $d_F = 1.16$ for $F = 0.92$. The fractal dimension thus increases as the motion becomes more chaotic as is to be expected but is always close to 1. The fractal dimension can also be calculated by direct-bin counting,[10] which is much more time consuming. We attempted to use an interpolation procedure to represent the Poincaré mapping for this purpose. To test the accuracy of the interpolation the Jacobian of the mapping was evaluated at each position of the phase point. For most points the small value of the Jacobian occurs despite much larger entries in the Jacobian matrix. In addition, the mapping is sometimes discontinuous where nearby points in phase space are mapped to different wells of the "pinning potential" (i.e., different wells of $\sin\phi$). For these reasons we were not able to find an interpolation scheme which could reliably yield the correct Jacobian over the entire range of interest in phase space. In reverting to direct integration of the differential equation for the Poincaré mapping, in conjunction with box counting algorithms for the fractal dimension, computer-time limitations restricted the degree to which convergences could be checked. Nevertheless, our results do seem to bear out the Kaplan-Yorke conjecture. For example, at $R = 0.5$, $\omega = 0.09$, and $F = 0.91$ we obtained $d_F \simeq 1.21$ (compared to 1.189 from Lyapunov exponents). It was found that the fractal dimension of the strange attractors tended to be larger, the smaller the value of R/ω, i.e., the smaller the dissipation per cycle).

The Kaplan-Yorke conjecture was also checked for these more fractured sets and seemed to hold as well. For example, at $R = 0.05$, $\omega = 0.1$, and $F = 1$ the solution is chaotic and the fractal dimension of the strange attractor was determined to be ~ 1.75 by bincounting compared to the value $d_F = 1.78$ obtained using the relationship to Lyapunov exponents.

VI. CONCLUSIONS

The results presented above show that the pendulum equation encompasses a wide range of behavior especially near the chaotic regime. We have observed two of the onset mechanisms predicted by use of one-dimensional maps, the period-doubling mechanism of Feigenbaum,[9] and the intermittency mechanism of Pomeau and Manneville.[6] We have not, as yet, been able to find a simple analytic form of the Poincaré map which reproduces the phase diagram or the varied type of onset behavior.

We are unaware of any studies that have probed the transition region for Josephson junctions—systems which we believe would display the features reported here. It would be of considerable interest to carry out such a study.

To date, no chaotic behavior has been seen in charge-density-wave systems. Our results indicate that if these materials are overdamped, as seems to be the consensus, no complicated behavior should be expected if Eq. (2) correctly describes the dynamics of the CDW. However, the bands of symmetry-broken solutions reported here may be related to the recently reported hysteresis phenomena.[5] This suggestion could be checked by relating the dc response in the presence of a large ac driving field to the occurrence of hysteresis.

ACKNOWLEDGMENTS

[1]D. E. McCumber, J. Appl. Phys. 39, 3113 (1968); see also the review article by N. F. Pedersen, *ibid.* 44, 5120 (1973).

[2]R. Y. Chiao, M. J. Feldman, D. W. Peterson, B. A. Tucker, and M. T. Levinsen, in *Future Trends in Superconductive Electronics—1978 (Charlottesville, Virginia,* Proceedings of the Conference in Future Trends in Superconductive Electronics, edited by B. S. Deaver, C. M. Falco, J. H. Harris, and S. A. Wolf (AIP, New York, 1978); Y. Taur and P. L. Richards, J. Appl. Phys. 48, 134 (1977).

[3]B. A. Huberman, J. P. Crutchfield, and N. H. Packard, Appl. Phys. Lett. 37, 750 (1980); see also N. F. Pederson and A. Davidson, *ibid.* 39, 830 (1981).

[4]See, for example, B. Joos, B. Bergersen, R. B. Goodings, and M. Plischke, Phys. Rev. B (in press).

[5]G. X. Tessema and N. P. Ong, Bull. Am. Phys. Soc. 27, 283 (1982).

[6]See the review articles by E. Ott, Rev. Mod. Phys. 55, 655 (1981); J.-P. Eckmann, *ibid.* 55, 643 (1981); R. H. G. Helleman, in *Fundamental Problems in Statistical Mechanics,* edited by E. G. D. Cohen (North-Holland, Amsterdam, 1980) pp. 165−233.

[7]M. Hénon and Y. Pomeau, in *Turbulence and the Navier Stokes Equation,* Vol. 565 of *Lecture Notes in Mathematics,* edited by A. A. Dold and B. Eckmann (Springer, Berlin, 1976), p. 29; D. Ruelle, *ibid.,* p. 146.

[8]P. Holmes, Philos. Trans. R. Soc. London 292, 419 (1979).

[9]M. J. Feigenbaum, J. Stat. Phys. 19, 25 (1978).

[10]D. A. Russell, J. D. Hanson, and E. Ott, Phys. Rev. Lett. 45, 1175 (1980); J. L. Kaplan and J. A. Yorke, in *Functional Differential Equations and Approximation of Fixed Points, Vol. 730 of Lecture Notes in Mathematics,* edited by H.O. Peitgen and H. O. Walther (Springer, New York, 1979), p. 228; H. Mori, Prog. Theor, Phys. 63, 1004 (1980).

[11]P. A. Lee, T. M. Rice, and P. W. Anderson, Solid State Commun. 14, 703 (1974).

[12]T. M. Rice, S. Whitehouse, and P. Littlewood, Phys. Rev. B 24, 2751 (1981).

[13]A. Zettl and G. Grüner, Phys. Rev. B 25, 2081 (1982).

[14]G . Grüner, A. Zawadowski, and P. M. Chaikin, Phys. Rev. Lett. 46, 511 (1981).

[15]A. H. MacDonald and Michael Plischke (unpublished).

[16]See F. M. Izrailev, M. J. Rabinovich, and A. D. Ugodnikov, Phys. Lett. 86A, 321 (1981) for a discussion of the relation between fractal dimensionality and mappings.

[17]B. V. Chirikov, Phys. Rep. 52, 263 (1979).

[18]C. M. Zaslavsky, Phys. Lett. 69A, 145 (1978).

[19]G. Benettin, L. Gulgani, and J.-M. Strelcyn, Phys. Rev. A 14, 2338 (1976).